Suitability of the Coralline Alga Clathromorphum compactum as an Arctic Archive for Past Sea Ice Cover

Natasha Leclerc, Jochen Halfar, Steffen Hetzinger, Phoebe Chan, Walter Adey, Alexandra Tsay, Eric Brossier, Andreas Kronz

Paleoceanography and Paleoclimatology

RESEARCH ARTICLE
10.1029/2021PA004286

Suitability of the Coralline Alga *Clathromorphum compactum* as an Arctic Archive for Past Sea Ice Cover

Natasha Leclerc[1], Jochen Halfar[2], Steffen Hetzinger[3,4], Phoebe T. W. Chan[5], Walter Adey[6], Alexandra Tsay[7], Eric Brossier[8], and Andreas Kronz[9]

[1]Department of Earth Sciences, University of Toronto, Toronto, ON, Canada, [2]Department of Chemical and Physical Sciences, University of Toronto Mississauga, Toronto, ON, Canada, [3]GEOMAR Helmholtz-Zentrum für Ozeanforschung Kiel, Kiel, Germany, [4]Christian-Albrechts-Universität zu Kiel, Institut für Geowissenschaften, Kiel, Germany, [5]Villefranche-sur-Mer Oceanographic Laboratory (LOV), Sorbonne University, Villefranche-sur-Mer, France, [6]Department of Botany, Smithsonian National Museum of Natural History, Washington, DC, USA, [7]Department of Earth Sciences, University of Geneva, Geneva, Switzerland, [8]Association Nord-Est, Lanton, France, [9]Geowissenschaftliches Zentrum, Universität Göttingen, Göttingen, Germany

Key Points:

- Annual proxy anomalies from growth increments and Mg/Ca ratios in calcareous algae were compared to satellite sea ice concentrations
- Algal growth anomalies most significantly correlated to sea ice concentrations at sites with medium wave exposure and >5 months sea cover
- Downsampled to 5-year averages, correlations are strengthened and can capture summer sea ice variability better than annual averages

Supporting Information:

Supporting Information may be found in the online version of this article.

Correspondence to:

N. Leclerc,
natasha.leclerc@mail.utoronto.ca

Citation:

Leclerc, N., Halfar, J., Hetzinger, S., Chan, P. T. W., Adey, W., Tsay, A., et al. (2022). Suitability of the coralline alga *Clathromorphum compactum* as an Arctic archive for past sea ice cover. *Paleoceanography and Paleoclimatology*, *37*, e2021PA004286. https://doi.org/10.1029/2021PA004286

Received 28 APR 2021
Accepted 12 NOV 2021

Author Contributions:

Data curation: Jochen Halfar, Phoebe T. W. Chan, Alexandra Tsay, Eric Brossier, Andreas Kronz
Formal analysis: Jochen Halfar, Steffen Hetzinger, Phoebe T. W. Chan
Funding acquisition: Jochen Halfar, Steffen Hetzinger
Methodology: Jochen Halfar, Eric Brossier
Project Administration: Jochen Halfar
Resources: Walter Adey, Eric Brossier
Supervision: Jochen Halfar
Writing – review & editing: Jochen Halfar, Steffen Hetzinger, Phoebe T. W. Chan, Walter Adey

Abstract Arctic sea ice cover has been steeply declining since the onset of satellite observations in the late 1970s. However, the available annually resolved sea ice data before this time are limited. Here, we evaluated the suitability of annual trace element (Mg/Ca) ratios and growth increments from the long-lived annual increment-forming benthic coralline red alga, *Clathromorphum compactum,* as high-resolution sea ice cover archive. It has previously been shown that the growth of *C. compactum* is strongly light controlled and therefore greatly limited during the polar night and underneath sea ice cover. We compare algal data from 11 sites collected throughout the Canadian Arctic, Greenland, and Svalbard, with satellite sea ice data. Our results suggested that algal growth anomalies most often produced better correlations to sea ice concentration than Mg/Ca ratios or when averaging growth and Mg/Ca anomalies. High Arctic regions with persistently higher sea ice concentrations and shorter ice-free seasons showed the strongest correlations between algal growth anomalies and satellite sea ice concentration over the study period (1979–2015). At sites where ice breakup took place before the return of sufficient solar irradiance, algal growth was most strongly tied to a combination of solar irradiance and other factors such as temperature, suspended sediments, phytoplankton blooms, and cloud cover. These data are the only annually resolved in situ marine proxy data known to date and are of utmost importance to gain a better understanding of the sea ice system and to project future sea ice conditions.

Plain Language Summary Natural layered structures such as tree rings and mollusk shells' growth layers archive environmental data in their rings or layers as they grow. A lesser known and emerging environmental archive is the coralline red algae species, *Clathromorphum compactum*, that lives on the Arctic and North Atlantic seafloor (10–30 m deep). It grows on solid substrate by forming a new calcified layer of growth every year, ultimately building up dome-like crusts over tens or hundreds of years. Different thicknesses of their annual layers depend on ocean temperature and sunlight availability. Because sea ice forms under cold conditions and blocks sunlight from reaching the sea floor, we hypothesized that growth also responds to sea ice conditions. Here, we evaluated the relationship between algal layer thicknesses and/or magnesium chemistry to sea ice data derived from satellite images at 11 sites. Strong relationships between algal growth and sea ice cover were found at exposed sites with longer seasonal-ice cover duration. Recent reductions of sea ice in certain regions have weakened the growth-sea ice relationship. A deeper understanding of past ice conditions can provide extremely valuable data for climate models to more accurately predict future sea ice scenarios.

1. Introduction

1.1. Sea Ice Effects on Global Climate Change and Lack of Long-Term High-Resolution Sea Ice Records

Summer sea ice extent has declined by 12.9% per decade since 1979 relative to the 1981–2010 average (Cavalieri & Parkinson, 2012; Comiso et al., 2017). This alarming rate of decline has potentially devastating impacts on Arctic ecosystems, and destabilizing effects on ocean circulation, global climate, and human populations due to the connection of sea ice to multiple feedback mechanisms including the ice-albedo feedback (Meier et al., 2014). However, current climate model projections are unable to fully capture annual sea ice variability and often underestimate the amount of sea ice decline due to a limited understanding of the internal and anthropogenic

processes driving sea ice loss (Ding et al., 2017). Models that project future climate scenarios currently utilize multiple short past sea ice data sets and sea ice-related variables, although more data sets from variable contexts are required to fine-tune model predictions. The sea ice records with the highest temporal and geographical resolutions are derived from satellite data sets providing almost daily global coverage back to 1979. Sea ice records that extend further back than 1979 are made from aggregated data sets with lower geographic coverages and temporal resolutions. Sources include stations, fishing, shipping, navy, research vessels, experiments, exploration expeditions, buoys, and historical data sources (for references, see e.g., Polyak et al., 2010; Worley et al., 2005). However, these data sets are spatially and temporally discontinuous. For instance, historical observations were biased toward the ice margins due to the constraints of penetrating pack ice. In addition, whale and seal hunting data sources excluded internal pack ice regions since marine life is typically more abundant along ice margins (e.g., Hill & Jones, 1990; Mahoney et al., 2011; Walsh et al., 2017).

1.2. Paleo-Sea Ice Proxies: Strengths and Limitations

Proxy information can yield sea ice information from less accessible internal sea ice regions and further back in time. Tree-ring proxy records and archives like lake sediments and ice cores from ice sheets can provide information on thermal conditions affecting sea ice formation and melt (for references, see e.g., Kinnard et al., 2011) but are remote from sea ice regions and may only yield limited information on the dynamics of sea ice. Meanwhile, marine proxies from sediment cores provide better information on sea ice dynamics that can extend back millennia, some records reaching back to the Miocene and Pliocene (Knies et al., 2014; Stein et al., 2016). The highly branched isoprenoid biomarker with 25 carbon atoms (IP25) found in ocean sediments can establish the presence or absence of seasonal sea ice as it is originally synthesized by diatoms living in the brine channels of first-year sea ice (Belt et al., 2007), while the semi-quantitative open-water phytoplankton-IP25 index (PIP25) can further indicate the concentration of sea ice cover and changes in distribution (Belt, 2019; Köseoğlu et al., 2018; Müller et al., 2011; Stein & Fahl, 2013). However, regional sedimentation rates are a limiting factor for proxies based on ocean sediment cores, yielding sub-decadal resolution data only in the best situations with interpolated 2-year to 5-year resolutions (Backman et al., 2004; Belt et al., 2012; Ran et al., 2011; Sicre, Jacob, et al., 2008; Sicre, Yiou, et al., 2008). Further, the use of assemblage analyses based on the identification and quantification of diatoms, foraminifera, ostracods, and dinoflagellate cysts (i.e., dinocysts) can also be challenging due to differential preservation of silica and calcareous-walled microfossils (e.g., Belmecheri et al., 2009; Bidle & Azam, 1999; Sexton & Wilson, 2009) and due to their presence in both perennial and seasonal sea ice cover environments, which are helpful to indicate presence but not duration of sea ice cover (Gemery et al., 2017; Kucera et al., 2005; Seidenkrantz, 2013). Since all sea ice proxies are geographically and temporally limited, a network of proxy records is needed to capture the full extent of spatial and temporal variability of sea ice dynamics and thermodynamics in the Arctic (Kaufman, 2009). Accordingly, high-resolution proxies that provide annual or seasonal sea ice information for the past millennia are necessary to calibrate climate models that project future sea ice behavior.

1.3. The Coralline Red Alga Sea Ice Proxy

An emerging archive for Arctic sea ice conditions is the coralline red algae species *Clathromorphum compactum* (Halfar et al., 2013; Hetzinger et al., 2019), a calcifying alga that grows ubiquitously in nearshore arctic and subarctic environments including the North Atlantic and the Bering Sea where rock and boulders cover the shallow benthic seafloor (Adey, 1965; Adey et al., 2013). *C. compactum* produces tree-ring-like annual growth increments in their calcified ($CaCO_3$) skeletons that are high in magnesium (Adey et al., 2013) (Figure 1). These slow-growing and long-lived algae can grow upwards of 600 years (Halfar et al., 2013). As they grow, they deposit layers of calcified cells in varying sizes and cell wall thicknesses that result in increments of lighter and darker bands (Foster, 2001). Experimental tank studies of *Clathromorphum* sp. have shown that their growth is highly dependent on both sunlight and temperature (Adey, 1970; S. Williams et al., 2018). Additionally, the variability of magnesium to calcium ratios (Mg/Ca) found in *C. compactum*'s annual growth layers is cyclical and strongly correlates with seasonal changes in surrounding sunlight availability and temperature (S. Williams et al., 2018). *C. compactum* produces its normal range of tissues with similarly complex high-magnesium calcitic wall structures both in the light and in the dark. However, growth is dependent upon the production and storage of photosynthate. Growth and calcification can occur for at least two months in the dark, at which point it ceases, following the exhaustion of stored photosynthate (S. Williams et al., 2018). The crust can exist for long periods

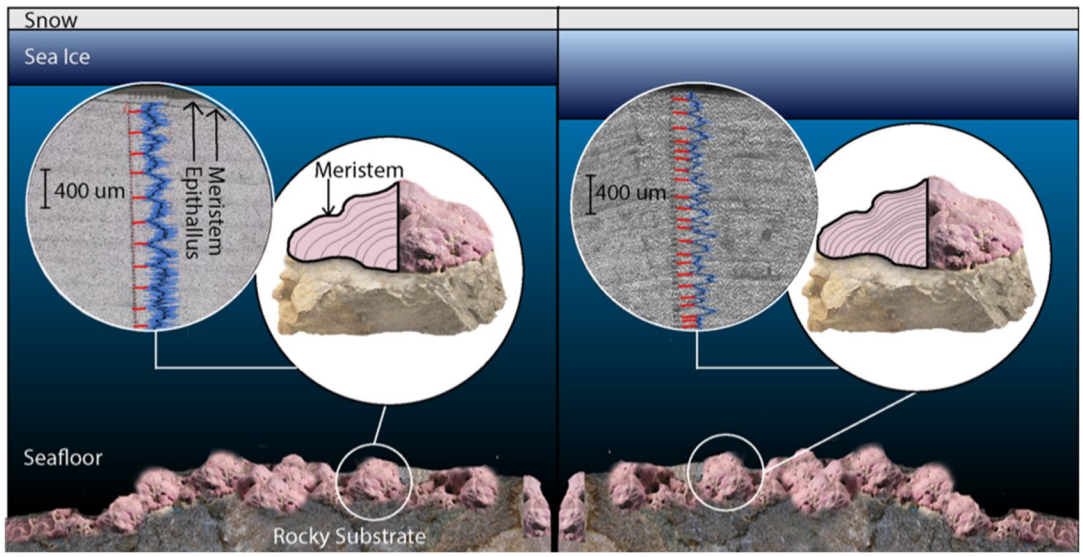

Figure 1. Schematic representation of relationship between length of sea ice cover and *C. compactum* growth and Mg/Ca ratios. Left panel indicates shorter duration of thin sea ice cover and thicker growth increments in depicted cross-section. Right panel indicates longer period of thick sea ice cover and consequently thinner algal growth increments. Mg/Ca ratios (blue), superimposed on high-resolution image of internal growth increments, are cyclical on annual timescales and match annual growth rates. Annual Mg/Ca minima are indicated with red lines and line-up with darker slow growth (winter) $CaCO_3$ layers. The meristem, typically, lying 5–10 cells below the algal surface is where algal growth and calcification occur. The overlying epithallus, weakly calcified and often grazed by molluscs, is ephemeral and location of most photosynthesis. Calcified tissue underlying meristem, the perithallus, builds up annual increments that provide multiannual proxy data.

without light, growth, or photosynthesis, and growth will resume with the return of new light for photosynthesis. Furthermore, growth rates have been shown to vary according to latitude and regional sunlight access (Halfar et al., 2013). In particular, growth rates are higher in coastal Maine (43°N) (400 μm/yr), as compared to southern Labrador (52°N) (240 μm/yr), and the Canadian Arctic Archipelago (73°N) (61 μm/yr) (Halfar et al., 2013). As growth and Mg/Ca ratios of *C. compactum* have been shown to be stimulated through photosynthesis, blocking of sunlight by seasonal sea ice cover has been hypothesized to reduce the widths of annual growth increments and reduce annual Mg/Ca ratios.

It has previously been shown that a combination of normalized growth rates and Mg/Ca ratios (i.e., algal anomalies) significantly inversely correlated with satellite-derived sea ice concentrations near algal collection sites in Arctic Bay (Nunavut) and the Kingitok Islands (Labrador) in Canada (Halfar et al., 2013). This suggested that when there was a longer duration of higher sea ice concentrations, less light reached the seafloor during the year, producing less growth (thinner increments) and reduced Mg incorporation (lower Mg/Ca ratios). Furthermore, a recent proxy time series of *C. compactum* from Svalbard, Norway, showed significant correlations between algal anomalies and regional sea ice concentration data and other Arctic sea ice proxy reconstructions, which demonstrated a reduction of sea ice and a general warming trend in Svalbard over the 20th century (Hetzinger et al., 2019).

To assess the robustness of sea ice proxies, fundamental questions regarding their strengths and weaknesses and the geographic and temporal contexts in which each proxy can be applied must be answered (De Vernal et al., 2013). While the above-mentioned studies have established the potential for *C. compactum* to be used for sea ice reconstruction, the strengths and weaknesses of the algal anomaly sea ice proxy have not been assessed in a multi-site comparison across the Arctic landscape. Furthermore, while the combination of Mg/Ca ratios and growth increment data has been correlated to sea ice concentration, it has not been established if both equally show a relationship or if growth alone could be used exclusively to compare to sea ice conditions. In this study, we investigate 30 *C. compactum* samples across 11 sites encompassing Svalbard (Norway), Western Greenland, Eastern Labrador (Canada), and multiple locations in Nunavut (Canada) (Figure 2). Their individual relationships to regional sea ice conditions were evaluated by the degree of correlation significance to satellite-derived sea ice concentration data sets, ice charts, and satellite images.

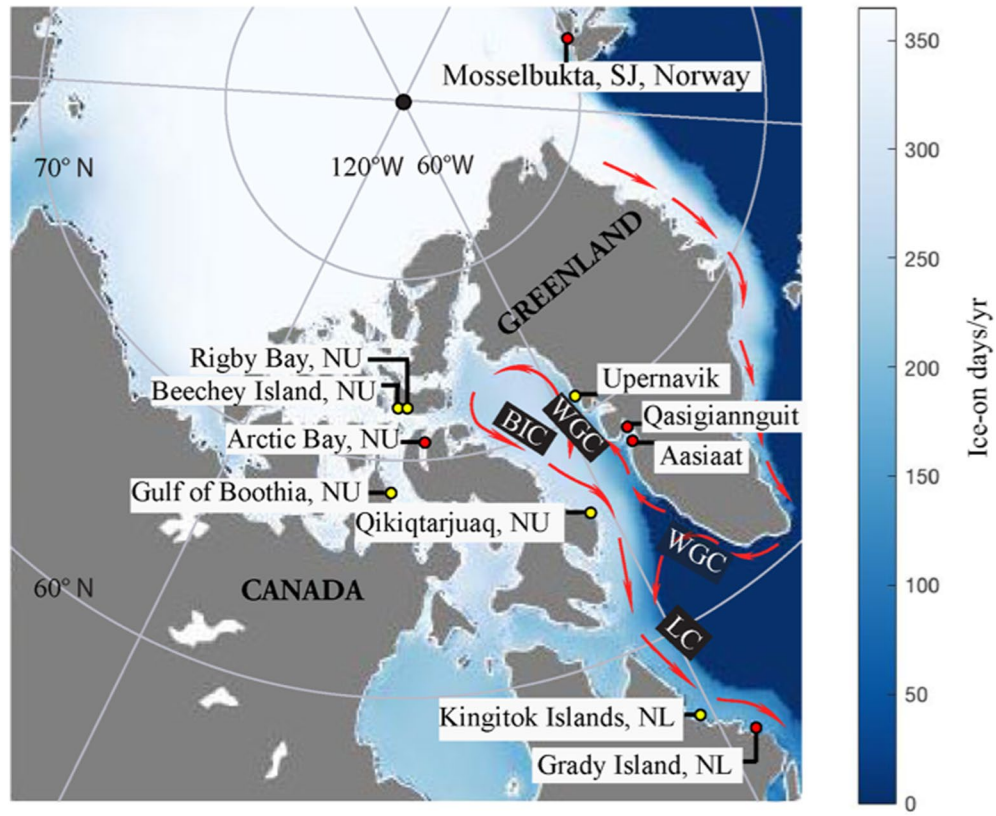

Figure 2. Studied arctic and subarctic *C. compactum* collection sites in Nunavut (NU) and Labrador (NL) in Canada, Greenland, and Svalbard (SJ) in Norway. Yellow dots indicate sites with significant relationships between summer sea ice concentration (SIC_{SUMMER}) and algal growth while red dots indicate sites with insignificant relationships that also tend to have shorter durations of ice cover near the ice margin. Average number of ice-on days with >15% ice cover over study period (1979–2015) shown graded from white (365 days) to dark blue (0 days). Currents depicted in black boxes: West Greenlandic Current (WGC); Labrador Current (LC) and; Baffin Island Current (BIC). Data source: daily NSIDC sea ice concentration data set 25-km resolution.

2. Materials and Methods

2.1. Sample Collection and Preparation

Live specimens of *C. compactum* were collected in 2008, 2010, 2011, 2014, and 2016, via SCUBA from 10 to 20 m depth (Figure 2, Table 1). Samples were cut along the axis of growth to expose growth layers with an Isomet precision saw. Samples were then polished with 9, 3, and 1 µm diamond-polishing suspension solutions on a Struers Labopol polishing disk and placed in an ultrasonic bath between polishing steps to remove adhering media. Sample cross-sections were imaged with an Olympus VS-BX reflected light microscope and automated stage using Geo.TS software (Olympus Soft Imaging Systems) that generated photomosaics of imaged area. From these images, the samples providing the longest records, regular growth, and presenting the least disruptions (e.g., cracks, disrupted growth, or conceptacles–reproductive structures of the alga) were selected for geochemical analysis. Samples were also inspected to ensure a visible meristem and epithallus—the growing edge and protective layer of the organism exposed to light—to confirm the deposition date of the first calcified perithallial layer beneath (i.e., at time of collection) (Figure 1).

2.2. Analytical Protocols for Mg/Ca and Growth Increment Measurements

Specimens from Svalbard, Greenland, Rigby Bay, Beechey Island, and the Gulf of Boothia collected in 2016 had laser ablation paths digitized on Geo.TS and path coordinates transferred to an NWR 193 UC laser ablation inductively coupled plasma mass spectrometer (LA-ICP-MS) system coupled with an Agilent 7900 quadrupole

Table 1
Sample Information for This Study and Time Period Compared to Satellite Records

Site	Latitude/Longitude	Sample ID	Measurement transects/sample	Period analyzed
Svalbard, Norway				
Mosselbukta	79°55'37.0"N	Sv1	2	1979–2014↓
	15°54'07.9"E	Sv18	1	1979–2015
		Sv28	2	1979–2015
		Sv47	1	1979–2015
		Sv90	2	1979–2015
West Greenland				
Aasiaat	68°44'9.83"N	2016_1_19	2	1979–2015
	52°32'10.86"W	2016_1_46	2	1979–2015
Qasigiannguit	68°53'51.54"N	2016_4_2	2	1979–2015
	51°16'54.19"W	2016_4_29	2	1988–2015
Upernavik	72°23'2.94"N	2016_7_21	2	1979–2015
	55°31'50.77"W	2016_7_27	2	1979–2015
		2016_7_30	2	1979–2015
East Labrador, Canada				
Grady Island	53°47'60.00"N	10-18_18-20	2	1979–2008↓
	56°24'30.00"W	10-18_15-17	2	1978–2008↓
Kingitok Islands	55°23'53.88"N	Ki1	1	1979–2010
	59°50'48.12"W	Ki2	1	1979–2010
Nunavut, Canada				
Qikiqtarjuaq	67°2'17.52"N	2014_4_1	2	1979–2012↓
	62°14'56.76"W	2014_4_2	2	1980–2012↓
		2014_4_3	2	1979–2012↓
Gulf of Boothia	70°24'18.12"N	16_49_80	2	1979–2015
	91°50'39.3"W	16_49_131	2	1979–2015
Arctic Bay	73° 1'2p64"N	AB1	1	1979–2007
	85° 9'12.96"W	AB30	1	1979–2007
		AB31	2	1979–2007
Rigby Bay	74°33'37.50"N	16_22_11	2	1979–2015
	90° 1'54.48"W	16_22_39	2	1979–2015
		16_22_90	2	1979–2015
Beechey Island	74°42'54.46"N	16_24_2b	2	1979–2015
	91°47'29.35"W	16_24_15	2	1979–2015
		16_24_41b	2	1979–2015

Note. Downward arrows indicate that a 1-year lag was identified in the time series.

mass spectrometer at the University of Toronto's Earth Science Center. Measurements of Mg/Ca were obtained by conducting continuous laser ablation line scans at 5 µm/s speed, an aperture size of 10 × 70 µm^2, and 10 Hz pulse rate. Samples from Arctic Bay, Kingitok Islands, and Qikiqtarjuaq, collected in 2008, 2011, and 2014 respectively, were analyzed for Mg/Ca using a JEOL JXA 8900 RL electron microprobe at the University of Göttingen with acceleration voltage of 10 kV, beam current of 12 nA, and spot diameter of 3.5 µm with a spacing of 10 µm between measurements along the axis of growth (for details of method, see Halfar et al., 2013). Samples collected from Grady Island in 2010 were analyzed at the University of Mainz, Germany in the Earth System Science Research Center using an Agilent 7500 quadrupole-ICP-MS attached to a New Wave Research UP-213

laser ablation system. Ablation measurements were obtained with a 65 μm spot size along continuous transects, a 10 μm/s speed, 10 Hz pulse rate, laser energy density of 6 J/cm^2, and helium carrier gas. All elemental data were calibrated with NIST SRM 610 standard (see details in Hetzinger et al., 2011). Resulting Mg/Ca data for all analyzed specimens was down-sampled to 12 measurements/year resolution with AnalySeries software (Paillard et al., 1996). When two measurement transects were taken from a sample, annual growth increment widths and Mg/Ca ratios were averaged between transects and were compared to aid in the construction of age models. Growth increment widths were calculated by measuring the distance between the time-stamped laser ablation measurements or electron microprobe spot measurements of two sequential Mg/Ca minima representing the space of 1 year (red lines, Figure 1). After the completion of age models, annual growth increments and Mg/Ca measurements from all specimens within an individual site were averaged, in order to better isolate the climate signal at each site. Both growth increment and Mg/Ca measurements were normalized into unitless anomalies. Annual growth increment and Mg/Ca anomalies were evaluated separately and also averaged to produce combined algal proxy anomalies.

2.3. Satellite Data Sets and Spatial Correlations

Combined algal anomalies were linearly regressed against monthly and annually averaged sea ice concentrations (SIC) from the gridded National Snow & Ice Data Center (NSIDC) Sea ice Concentration Data Set (Version 3) that extend from 1979 to present (https://nsidc.org/data/g02202; Peng et al., 2013). These data were obtained through passive microwave sensors Nimbus-7 SMMR and DMSP SSM/I-SSMIS that measure surface brightness converted to 25 × 25 km^2 gridded sea ice concentrations via algorithms that also reduce the bias between different instruments used during the satellite era (Meier et al., 2017; Peng et al., 2013). Due to some sites being incorporated in gridded cells classified as land, SICs from the cells surrounding all collection sites were averaged when calculating correlations between regional sea ice conditions (75-km resolution) and algal anomalies. Data gaps were found from December 1987 to January 1988 and were therefore not used in the calculation of annual SIC averages. Daily NSIDC SIC 25-km resolution data set was used to determine the average number of ice-free days (<15%) per year for the 75-km gridded area around each of the collection sites. SIC monthly means that significantly inversely correlated with algal anomalies ($p < 0.05$) were pooled together by averaging these months' SIC, which were then statistically regressed against algal anomalies. Regional maps displaying spatial linear regression analyses of algal anomalies and sea ice concentrations were generated with MATLAB version R2018a and m_map add-on. Sea surface temperatures from HadISST data set at a 1° resolution (Rayner et al., 2003) were also used to conduct linear regression statistics between algal anomalies and nearest 1° grid cell values (https://www.metoffice.gov.uk/hadobs/hadisst/). The Norwegian Meteorological Institute's archived nearly daily sea ice charts (1997–2015) for the Fram Strait and Svalbard regions (https://cryo.met.no/archive/ice-service/icecharts/quicklooks/) and satellite imagery from NASA Worldview (https://worldview.earthdata.nasa.gov) were used to examine sea ice concentrations at a higher spatial resolution than the NSIDC data set. Satellite cloud fraction cover data (EUMETSAT/CMSAF; 0.25° resolution) obtained from KNMI Climate Explorer (climexp.knmi.nl), and monthly chlorophyll α concentrations (MOSISA_L3mCHL v2018; 4-km resolution) were obtained through NASA Earth Data's tool Giovanni (https://giovanni.gsfc.nasa.gov). Linear regression tests were run between algal anomalies and monthly or annual SIC averages and durations of ice-free season for all sites (75-km resolution). Multiple months' SICs were averaged when algal anomalies correlated with more than one monthly SIC (SIC_M), which were restricted to the highest solar irradiance season of May to October (Adey et al., 2013). SIC_M means were then regressed against algal anomalies. The significances of all linear regressions were evaluated by calculating the p-value with an ANOVA test; all tests with p values less than 0.05 were deemed significant correlations when Pearson r values were positive or negative depending on the relationship with algal growth (see Table S1 in Supporting Information S1 for summary of relationships).

3. Results

3.1. Annual Mean Mg/Ca and Growth Increment Comparison

Growth increments and Mg/Ca ratios (Figure S4 in Supporting Information S1) were independently linearly regressed against annual sea ice concentrations (SIC_A) to determine whether they equally contributed to correlations between SIC_A and the combined algal anomalies. The results revealed that both growth increments and combined algal anomalies had the strongest significant negative correlations with SIC_A at four sites (Figure 3).

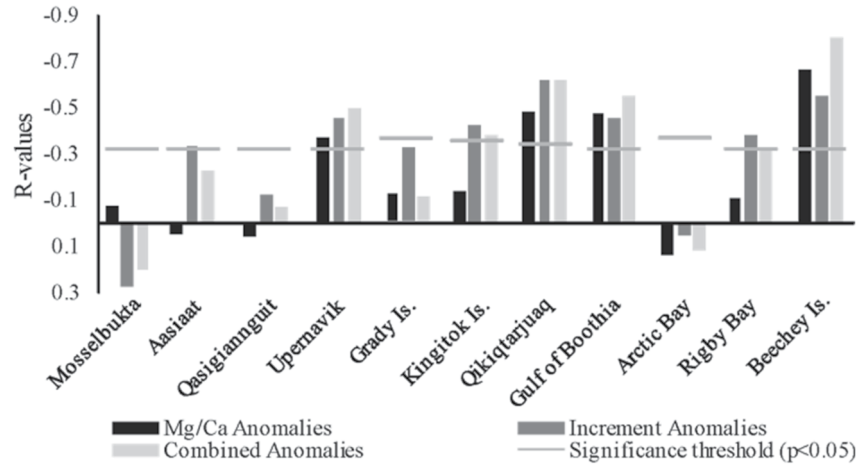

Figure 3. Mg/Ca, growth increment, and combined algal anomalies regressed against SIC_A (1979-sample collection date). Horizontal lines indicate threshold for significance ($p < 0.05$).

However, growth increment anomalies alone outperformed the other proxies by producing significant negative correlations with SIC_A at seven sites compared to five and four for combined algal anomalies and isolated Mg/Ca anomalies, respectively (Figure 3). Since the results suggest a more robust relationship between growth increments and SIC_A at most sites, the rest of the results and discussion will focus only on the growth increment anomaly results.

3.2. Relationship Between Sea Ice and Algal Growth Anomalies

Linear regression results suggested that algal growth anomalies at 7 out of 11 sites had significant negative correlations with SIC_A ($p < 0.05$), 2 of which tested as significantly positive correlations with the annual durations of the ice-free period (i.e., days with <15% SIC; Table 2). Algal anomalies from 8 sites significantly inversely correlated with at least 1 month of the monthly resolved NSIDC data set (SIC_M) during the study period (Table 2). Among these, Aasiaat showed a negative correlation to May only, when sea ice typically breaks up in this location. While the annual SIC averages were used for comparison (SIC_A), previous studies suggested that growth resumes after a winter shutdown, once solar irradiance reaches the seafloor when sea ice breaks up (Adey et al., 2013). Accordingly, summer month SIC averages (May–October) were isolated from the annual data set and compared to growth anomalies. Six sites had growth anomalies that significantly correlated with SIC_{SUMMER}. Growth anomalies with non-significant correlations or low significance to regional SIC tended to be from sites closer to the ice margin with longer ice-free periods (red dots; Figure 2). In comparison to annual means, linear regression results of 5-year running means were more significant (i.e., lower *p*-values), especially in regions with shorter ice-free periods, at the majority of sites (N5; Table 2). Algal growth anomaly time series from individual sites further show the synchrony with SIC_{SUMMER} at most sites (Figure 4).

3.3. Spatial Patterns of Sea Ice Correlation

Figure 5 illustrates that most sites had inverse relationships with regional SIC_{SUMMER}. Algal growth anomalies from sites with the most significant negative correlations with SIC_{SUMMER} tended to exhibit a strong regional relationship with large Arctic areas. For example, Beechey Island had the strongest negative correlations around the collection site, but also had strong correlations with most of the Canadian Arctic Archipelago, likely owing to similar regional sea ice dynamics (Melling, 2002). On the Labrador coast, regional correlations around Kingitok Islands and Grady Island were influenced by the Labrador Current with negative correlations extending to the west coast of Greenland. The Baffin Island current seemed to be mostly affecting the algal-sea ice relationship at Qikiqtarjuaq, while the West Greenlandic current seemed to have most of an effect on Upernavik algal anomalies.

Table 2
Results of Linear Regression Analysis Between Growth Increment Anomalies and Sea Ice Conditions (R- and p-Values)

Site	Mean SIC_A	Mean Ice-free days	Linear regression results between growth anomalies and sea ice variables															
			SIC_A (Jan-Dec)				SIC_M						SIC_{SUMMER} (May-Oct)				Ice-free days	
			R	p	$R_{(N5)}$	$p_{(N5)}$	Months ($p<0.05$)	R	p	$SIC_{M\ (N5)}$ ($p<0.05$)	$R_{(N5)}$	$p_{(N5)}$	R	p	$R_{(N5)}$	$p_{(N5)}$	R	p
Mosselbukta, NO	39%	217	0.27	0.1	0.01	0.95	**	**	**	**	**	**	0.18	0.27	-0.05	0.80	-0.004	0.98
Aasiaat, GL	36%	204	-0.34	0.04	-0.44	0.01	May	-0.40	0.02	May	-0.58	0.0004	-0.17	0.32	-0.23	0.19	0.14	0.41
Qasigiannguit, GL	45%	229	-0.13	0.46	0.03	0.86	Aug-Oct	-0.39	0.02	Aug-Oct	-0.68	0.00001	-0.21	0.20	0.06	0.76	0.001	0.99
Upernavik, GL	46%	218	-0.46	0.005	-0.49	0.004	Jun; Aug-Oct;	-0.45	0.005	May; Aug-Oct	-0.50	0.003	-0.41	0.01	-0.51	0.002	0.12	0.45
Grady Island, NL	38%	287	-0.30	0.10	-0.01	0.95	**	**	**	**	**	**	-0.24	0.19	-0.20	0.32	-0.11	0.56
Kingitok Islands, NL	44%	201	-0.42	0.015	-0.59	0.001	Jun-Jul	-0.44	0.01	May-Jul	-0.66	0.0001	-0.44	0.01	-0.66	0.0001	0.27	0.14
Qikiqtarjuaq, NU	67%	120	-0.54	0.001	-0.73	4.9E-06	Jul-Sep;	-0.66	2.1E-05	Jun-Aug; Oct	-0.81	4.4E-08	-0.59	0.0002	-0.78	3.5E-07	0.43	0.01
Gulf of Boothia, NU	88%	112	-0.46	0.004	-0.79	5.7E-08	Jun-Oct	-0.48	0.003	May-Oct	-0.78	5.4E-07	-0.48	0.003	-0.78	5.4E-07	0.33	0.04
Arctic Bay, NU	90%	190	0.06	0.77	0.47	0.02	**	**	**	**	**	**	0.04	0.85	0.37	0.07	-0.01	0.95
Rigby Bay, NU	82%	132	-0.38	0.02	-0.65	0.00004	Aug-Oct	-0.39	0.02	May-Jun; Aug-Oct	-0.70	4.7E-06	-0.37	0.02	-0.65	3.8E-05	-0.31	0.07
Beechey Island, NU	85%	130	-0.55	0.0004	-0.59	0.0003	May-Oct	-0.74	1.6E-07	May-Oct	-0.90	6.9E-13	-0.74	1.6E-07	-0.90	6.9E-13	-0.31	0.07

Note. Months falling between May and October that individually produced significant and negative correlations to algal growth anomalies are labeled under SIC_M: Months ($p < 0.05$). Monthly SIC that significantly inversely correlated to algal growth anomalies when downsampled to 5-year running means are labeled under $SIC_{M\ (N5)}$ ($p < 0.05$). All mean values were calculated for 1979 to year of collection. Significant correlations ($p < 0.05$) shaded orange. Five-year running mean comparison indicated by N5 subscript. Sites with no significant correlating months indicated with two asterisks (**). Positive correlation to SIC and negative correlations to mean ice-free days shaded in gray.

3.4. Algal Growth-Temperature Relationship

According to experimental results, *C. compactum* was expected to exhibit higher growth in warmer SST conditions; therefore, algal growth anomalies should positively correlate to SST to demonstrate the growth temperature dependence (S. Williams et al., 2018). Correlations of algal growth anomalies with SST_A and SIC_A were not significantly different (paired two-tailed *t*-test: d$f = 10$, $t = -2.09$, $p = 0.06$, CV = 2.23) owing to the thermal relationship between sea ice and SST at an annual resolution. SST_{SUMMER} correlated to algal growth anomalies at four sites, nearly half of the sites that SIC_{SUMMER} significantly correlated to. SST_{SUMMER} also produced weaker relationships to algal growth than did SIC_{SUMMER} (paired two-tailed *t*-test: d$f = 10$, $t = -2.64$, $p = 0.02$, CV = 2.23) (Tables 2 and 3, Figure S1 in Supporting Information S1). This indicated algal growth anomalies' strong seasonal sunlight dependence reflecting *C. compactum*'s primary growing season in the summer.

3.5. Temporal Variability of Algal-Sea Ice-Temperature Relationships

Temporal shifts in correlation between algal anomalies and SIC and SST were investigated through the generation of 10-year running correlations. The temporal shift in correlation over the past few decades indicated two overarching trends: (a) reduction of proxy strength in recent decades due to the rapid reduction of sea ice; (b) increasing proxy strength in recent years due to higher inter-annual sea ice variability (Figure 6). However, due to the short duration of records and thus low sample size, many of the correlations are not significant ($n = 10$/running correlation).

Algal anomalies in Aasiaat, Greenland, had strong correlations to SIC in the early record, followed by weaker correlations in the late record into the 2000s (Figure 6a). Notably, the late record is marked by increased inter-sample algal anomaly variability (Figure 4a). In addition, when comparing the relationship between SIC_{SUMMER} and growth time series (Figure 4b) and how it has changed through time at Qasigiannguit (Figure 6b), periods of low inter-annual SIC_{SUMMER} variability (1999–2015) produced algal anomalies that did not strongly correlate to sea ice records. Correlations with SIC_{SUMMER} were periodically stronger than SST_{SUMMER} in the earlier and mid-section of the satellite record, yet not significant; however, the relationship with temperature has increased

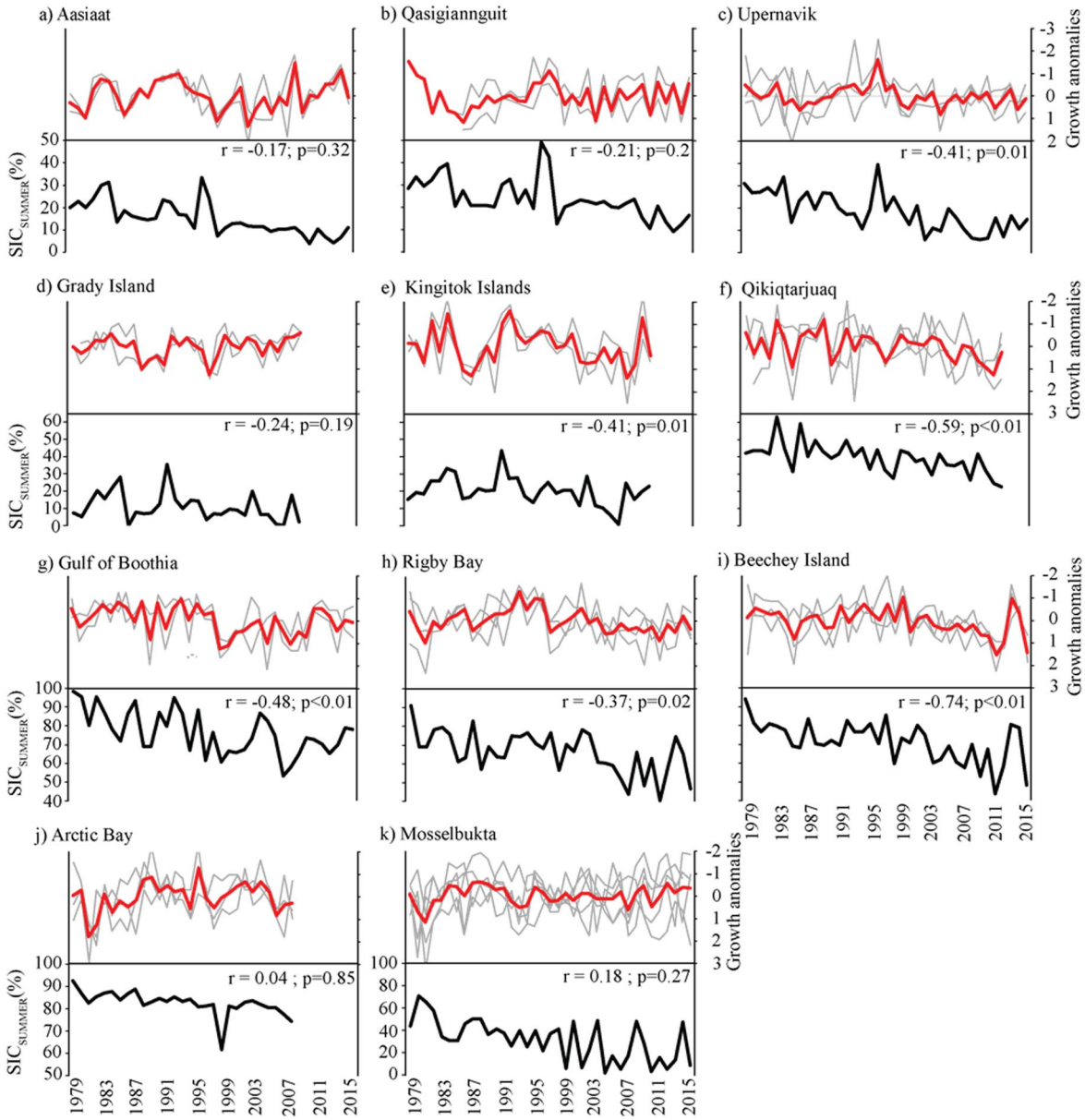

Figure 4. Algal growth anomalies (red) and SIC_{SUMMER} (black: May–October means) time series. Algal growth anomalies from individual samples in gray. Note that algal growth anomalies are presented on inverted axis.

since the early 2000s (Figure 6b). Upernavik also had stronger algal-sea ice relationships in the early record, which weakened in the 1990s when sea ice became completely absent in July after 1996 (Figure 6c). Kingitok Islands and Grady Island (Figures 6d and 6e) results showed that correlations with SIC and SST were stronger in the early record than in the late record. Kingitok Islands and Grady Island experienced a significant reduction of sea ice after 1995. Accordingly, correlations with SIC_{SUMMER} and SST_{SUMMER} were stronger before 1995 and correlations are generally weaker in recent years as temperatures have been relatively stable and cloud cover has reduced. On the other hand, Qikiqtarjuaq, Gulf of Boothia, Rigby Bay, and Beechey Island experienced a steady decline in SIC since the beginning of the satellite record but retained a higher concentration of sea ice for longer periods compared to other studied regions (Figure 4). Algal growth anomalies generally track the lower and higher ice years but cannot account for the full amplitude of sea ice variability and/or tend to have lower correlations during periods of low variability (Figures 4 and 6). Qikiqtarjuaq, Rigby Island, and Beechey Island correlations to SIC were stronger after the 1980s, a period marked by higher variability of sea ice and algal growth anomalies

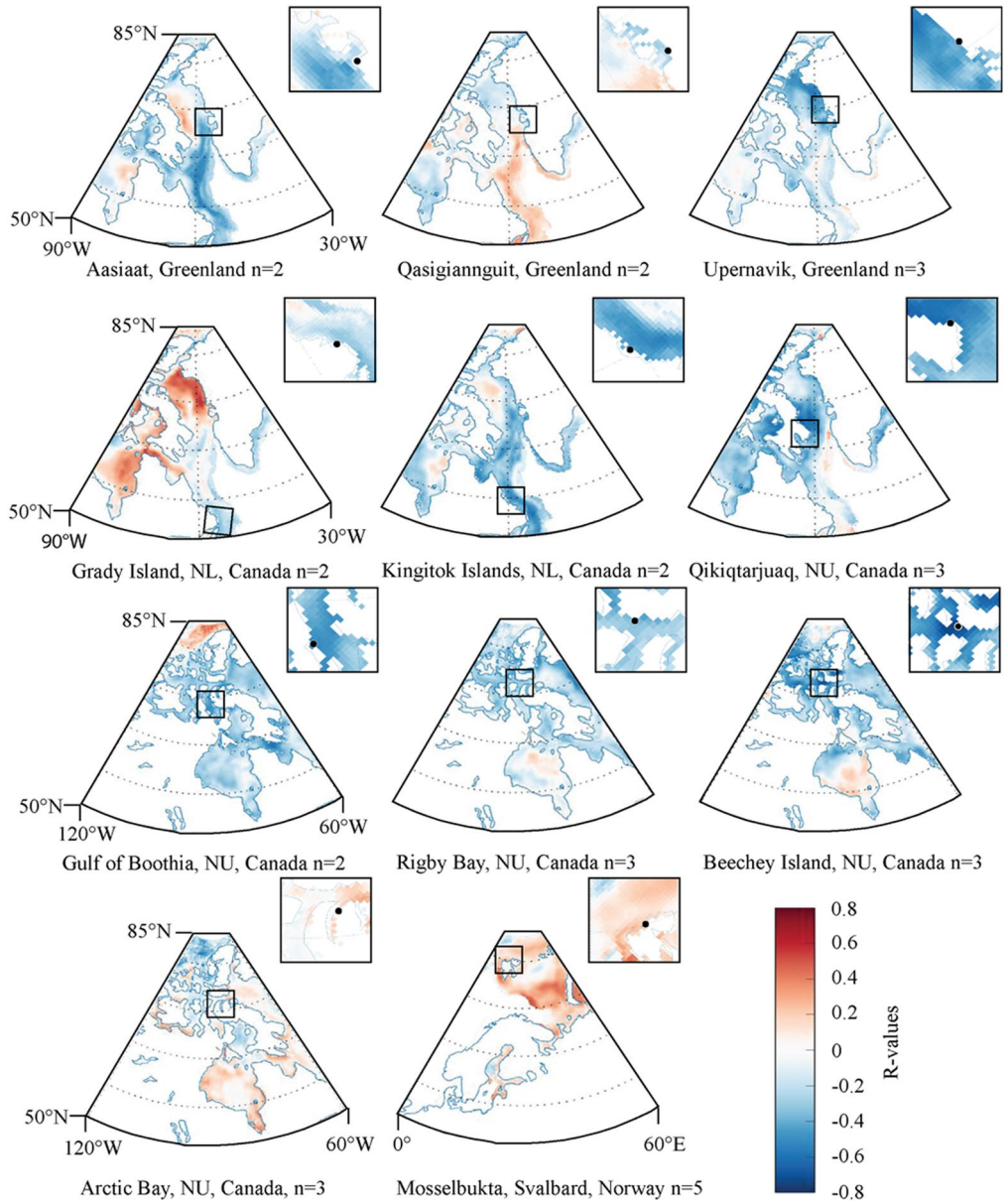

Figure 5. Spatial correlations between SIC_{SUMMER} and algal growth anomalies. SIC data retrieved from NSIDC Sea ice Concentration Version 3, monthly data sets. Spatial correlations calculated with Matlab mapping toolbox. Black dots in inset images indicate collection sites. Time series length varied depending on algal collection date: see Table 1.

(Figures 6f–6i). Similar to Qasigiannguit, correlations at Qikiqtarjuaq of growth anomalies to SST have strengthened while those to SIC have decreased (Figure 6f). In the Gulf of Boothia, correlations to SIC are strongest in the mid-record when SIC and algal growth anomalies have high inter-annual variability (Figures 4g and 6g).

3.6. Inter-Series Variability

Synchrony of growth anomalies between samples from the same site was measured by first conducting linear regression tests between algal anomaly time series sample pairs, and averaging *R*-values together to express a site's inter-series correlation (R_{bar}), a statistic often used to express synchrony in dendro- and sclerochronology (e.g., Butler et al., 2009). While inter-series correlations at the annual level were only significant at one site, inter-series correlations were significant at five sites when 5-year running averages were used (Figure 7).

Table 3
Results of Linear Regression Analysis Between Algal Anomalies and SST (R- and p-Values)

Site	Mean SST_A (°C)	Linear regression results between growth anomalies and SST						
		SST_A (Jan-Dec)		SST_M			SST_{SUMMER} (May-Oct)	
		R	p	Months (p<0.05)	R	p	R	p
Mosselbukta, NO	1.07	-0.24	0.15	Sep	0.44	0.006	-0.14	0.40
Aasiaat, GL	1.41	0.29	0.08	May	0.52	0.001	0.17	0.30
Qasigiannguit, GL	1.41	-0.07	0.70	**	**	**	0.05	0.75
Upernavik, GL	0.81	0.47	0.004	Aug-Sep	0.42	0.02	0.39	0.009
Grady Island, NL	2.49	0.27	0.14	**	**	**	0.08	0.68
Kingitok Islands, NL	1.14	0.31	0.08	Jul-Sep	0.51	0.003	0.44	0.01
Qikiqtarjuaq, NU	-0.63	0.47	0.005	Jul-Oct	0.53	0.0002	0.50	0.002
Gulf of Boothia, NU	-1.36	0.28	0.1	Jul	0.39	0.02	0.27	0.1
Arctic Bay, NU	-0.94	0.03	0.88	**	**	**	0.03	0.88
Rigby Bay, NU	-0.86	0.16	0.36	Sep	0.39	0.02	0.15	0.38
Beechey Island, NU	-1.01	0.57	0.0002	May-Oct	0.56	0.0003	0.56	0.0003

Note. Monthly SST falling between May and October that individually produced significant and positive correlations to algal growth anomalies are labeled under SST_M: "Months ($p < 0.05$)." Significant correlations ($p < 0.05$) shaded orange. Sites with no significant correlating months indicated with two asterisks (**). Negative correlations shaded gray.

4. Discussion

4.1. Influence of Runoff and Degree of Exposure on Algal-Ice Relationships

Sites that are significantly correlated with SIC_A and SIC_{SUMMER} tend to be in relatively exposed regions, away from glacial and fluvial runoff sources. As was suggested by Adey et al. (2015), these mid-exposure habitats in terms of currents and waves would likely yield the longest-lived *C. compactum* specimens, as they would be affected by low levels of sedimentation and enough grazers to remove sedimentary detritus on algal surfaces. Accordingly, growth may be more affected by temperature or overlying sea ice if it is not impeded by grazers and/or sediment accumulation. Sites that are relatively exposed include Beechey Island, Gulf of Boothia, Qikiqtarjuaq, Kingitok Islands, and Upernavik as they are situated on islands away from the coast or on peninsulas as opposed to embayments. The results from these sites (Figure 5) support the hypothesis that *C. compactum* growth anomalies respond firstly to local SIC conditions and, by association, secondarily to regional SIC conditions. Slightly less exposed sites include Rigby Bay, Aasiaat, and Qasigiannguit which are located near the mouth of exposed bays. Algal growth increments are likely recording very localized light variation when their locations are more secluded such as the Arctic Bay site in the Canadian Arctic Archipelago. Arctic Bay's distance to more dynamic sea ice regions in the archipelago is distinct from other sites investigated, leading to a low energy environment with possible increased sediment buildup on the algae, thereby lowering receipt of light.

Furthermore, *C. compactum* samples are collected in nearshore environments, environments that become increasingly vulnerable to higher sediment discharge with warming conditions and reduced sea ice (Teichert & Freiwald, 2014). Accordingly, diminishing correlations between algal growth anomalies and SST and/or SIC instrumental records may be enhanced in regions near sediment runoff. The results from Mosselbukta and Aasiaat suggest decreasing correlations with SIC, particularly noticeable in the 1990s into the early 2000s (Figures 6a and 6k) as SIC significantly declined. While instrumental data for runoff is not available for Mosselbukta, Svalbard, modeled runoff data suggested increasing runoff in recent decades (Lang et al., 2015; Möller & Kohler, 2018; van Pelt et al., 2016; Østby et al., 2017). Barium-calcium ratios (Ba/Ca) in coralline red algae have

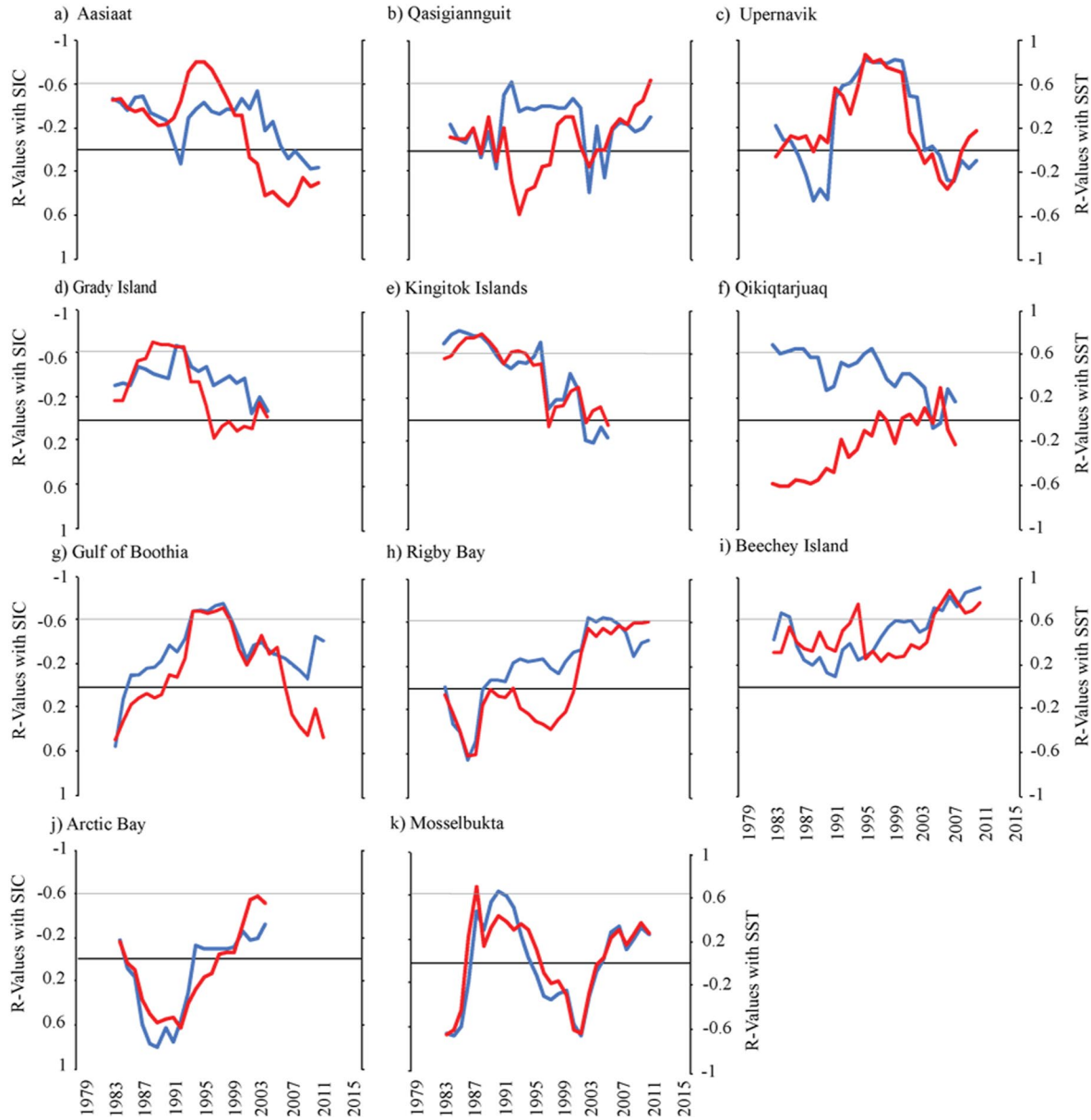

Figure 6. Results of 10-year running correlations achieved with linear regression between algal growth anomalies and mean SST_{SUMMER} and SIC_{SUMMER} (May–October). Red line represents correlations with summer SST, and blue line represents correlation with summer SIC. Gray horizontal line indicates 95% significance threshold.

previously been used to reconstruct variability in runoff in nearshore environments (Chan et al., 2011). More recently, a study on *C. compactum* Ba/Ca from Mosselbukta effectively suggested a drastic increase in runoff since the late 1980s (Hetzinger et al., 2021). This could have created more turbidity in the water column and less solar light transmission to the benthos, causing a recent reduction in increment widths in the Mosselbukta samples. The Aasiaat samples also exhibited a trend toward thinner growth increments in recent years, while reduction of SIC should have caused an increase in growth. Due to Aasiaat's proximity to the Jakobshavn glacier near Illullisat, Greenland, increased sedimentation may have also reduced increment widths.

4.2. Ice-On Duration Effect on Algal Response to Sea Ice Conditions

S. Williams et al. (2018) suggested that light plays a more significant role in *C. compactum*'s growth in warmer environments. While this may be true in ice-free regions with more balanced light and temperature controls, the

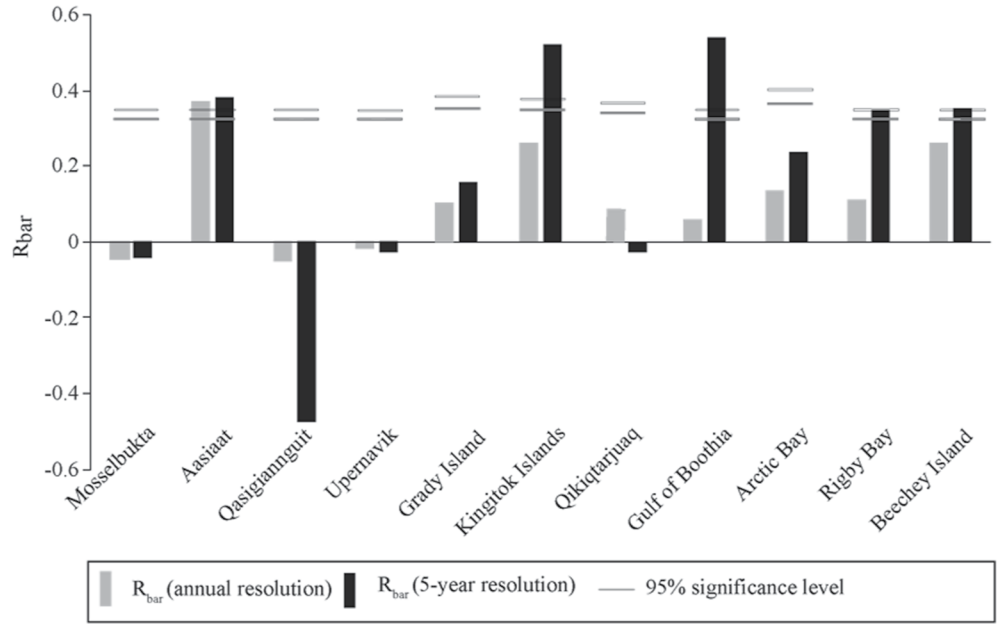

Figure 7. Inter-series correlation results (R_{bar}) at annual (gray) and 5-year average (black) resolutions with corresponding 95% significance level threshold (dark gray: annual resolution; light gray: 5-year average resolution).

results of this study showed that algal growth anomalies from regions with shorter ice-free seasons (i.e., shorter sunlight access) and lower sea surface temperatures (Tables 2 and 3) were better able to record light-inhibition by ice cover than regions near the ice margin with longer ice-free seasons (Figure 2, Table 3). Spatial correlation maps indicate that algal anomalies from the most affected sites have strong relationships with regional SIC and ocean currents (Figure 5). Currents play a significant role in sea ice dynamics (Warn-Varnas et al., 1991), causing similar sea ice conditions along them. Accordingly, these high correlation regions indicate which regions may yield future samples useful to reconstruct regional sea ice.

The results also suggest that recent reductions in sea ice have reduced the correlation between sea ice conditions and algal growth. Upernavik has witnessed ice-free Julys since 1997 following a positive Arctic Oscillation phase which continued to decrease multi-year ice coverage for years, after which algal growth correlations to sea ice and temperature appear to have both reduced (Figure 6c). After the late 1990s, algal growth increment variability was noticeably reduced, reflected also by low and stable sea ice concentrations (Figure 4c). However, algal growth anomalies did not always match regional sea ice variability suggesting that other factors may have affected algal growth variability. According to a recent study by He et al. (2019), cloud increased in the Upernavik region since the early 2000s. Previous work on the coralline red algae species *Lithothamnion glaciale*, found an inverse relationship between summer calcification and the previous winter's cloud cover in Scotland (Burdett et al., 2011). Therefore, while sea ice concentrations have reduced around Upernavik and produced a trend toward thicker growth increments, increased cloud cover may have counteracted the effect of the longer ice-free season by dimming sunlight access to the sea floor, thereby reducing the inter-annual variability (i.e., amplitude) of growth increments (Figure 4c), and the correlation between sea ice and algal growth (Figure 6c) in the last decade of the record.

Similarly, in the early satellite record, the Kingitok Islands have experienced increasingly longer ice-free seasons since the early 2000s. The reduction of sea ice may have disrupted the previously stronger sea ice relationship with algal growth. Results of 10-year running correlations show that SIC_{SUMMER} and SST_{SUMMER} correlations with algal growth anomalies declined in the 2000s likely as a result of the lengthening of the ice-free period (Figure 6e). In addition, local summer cloud cover has been declining (−2.65% per decade, 1982–2010) likely causing increased sunlight irradiance reaching algal specimens and consequently larger increments in lower SIC years and increased inter-annual variability of sunlight-driven growth.

On the other hand, Grady Island's algal growth anomalies weakly correlated with SIC_{SUMMER} and SST_{SUMMER} trends (Tables 2 and 3), but produced significant 10-year running correlations (Figure 6a), suggesting they responded to sea ice variability. Since linear regressions are sensitive to trends, the fact that algal growth anomalies showed a strong trend toward smaller increments in the 2000s while deteriorating sea ice conditions typically bolster the formation of larger increments suggested that factors other than SST and SIC limited algal growth in recent time. Comparisons between algal growth anomalies, regional phytoplankton productivity time series (Glen Harrison et al., 2013), and chlorophyll α concentration from MODIS/Aqua satellite records indicated that years with higher summer Chlorophyll α concentrations often occurred simultaneously with lower algal growth anomalies. Barium-calcium ratio and carbon isotopes time series derived from *C. compactum* have previously established the relationship between coralline red algae geochemistry (Ba/Ca and $\delta^{13}C$) and sea ice driven productivity variability (Chan et al., 2017). Due to the relationship between algal growth and light availability, it is likely that turbidity caused by large phytoplankton blooms may have affected the amplitude of algal growth anomalies especially in regions with longer ice-free seasons.

In addition, algal growth anomalies from regions that experienced significant reductions in sea ice cover may shift from being sea ice dependent to being temperature dependent, as exhibited by the Qasigiannguit and Qikiqtarjuaq samples. Previous studies examined the multi-centennial Mosselbukta algal time series and revealed a strong relationship between combined algal anomalies and sea ice cover from the early twentieth century to the early 2000s (Hetzinger et al., 2019), demonstrating that the algal sea ice proxy had a higher recording strength during periods and in regions of longer sea ice cover duration. Therefore, sea ice may have variable control on algal growth anomalies depending on the length of the open water season, when the annual solar insolation cycle, temperature, and other light inhibiting variables exert a stronger influence on algal growth, especially for sites closer to the margins of pack ice. On the other hand, shorter ice-free periods may limit the effect light inhibitors (excluding sea ice) have on annual algal growth anomalies.

4.3. Spatial Resolution Bias of the Satellite Record

Typically, the ice-free season is defined as less than 15% sea ice concentration (Wang & Overland, 2012), providing a warmer open water period when photosynthetic growth of *C. compactum* should be occurring (Adey, 1970; S. Williams et al., 2018). However, the data from this study suggested that *C. compactum* grew and recorded SIC during months with higher than 15% sea ice cover over the 75 km^2 gridded area (Figure 4). For example, regions such as Lancaster Sound near Beechey Island had the strongest negative correlation of all sites (Table 2, Figure 5), but has seldom recorded monthly means lower than 30% SIC over the study period. A 1° spatial resolution SIC time series provided by the KNMI Climate Explorer tool revealed that months with the strongest negative correlations at Beechey Island occurred during low SIC months (i.e., May–October), but SIC levels were rarely below 15% (Reynolds et al., 2002). Further, NASA satellite images showed ice breakup around Beechey Island by late July that was cleared of ice by early August (2002–2015) suggesting that the lack of correlation between ice-free day/year and algal growth anomalies (Table 2) may be caused by an inaccurate representation of local ice-free and ice-on days in the 75 km^2 gridded satellite cell. Further, some issues regarding early sensors and data homogenization (National Center for Atmospheric Research Staff, 2019) may have challenged the comparison of satellite-derived SIC to algal anomalies as early satellite imagery was unable to capture SIC in small channels and bays due to the presence of land within large 25 km^2 grid cells (Howell et al., 2009). This is particularly noticeable in the region around Arctic Bay, where satellite imagery showed some discrepancies in timing of ice formation and breakup between the secluded setting of Arctic Bay and the adjacent larger inlet which offered the nearest gridded SIC data (Figure S2 in Supporting Information S1).

4.4. Temporal Resolution of Algal-Ice Relationship

The measure of ice-free days consists of very high-resolution temporal data; however, algae likely start growing well before the database records <15% sea ice concentrations. Similarly, photosynthetic phytoplankton start blooming while the ice is thin, largely devoid of snow, and full of melt ponds (Massicotte et al., 2020), while daily satellite records would still record ice cover (<15%). This may explain why few correlations were found between annual growth anomalies and ice-free days. Though we were unable to quantify the role of ice thickness and snow thickness on *C. compactum* growth, these data suggest that ice and snow thicknesses play a role in algal growth variability. In addition, correlations with SIC were appreciably stronger when both growth increment and

SIC measurements were downsampled to 5-year running means (Table 2). *C. compactum*'s growth increments have previously been shown to correlate well to long-term regional sea ice decline over at least the past century (Halfar et al., 2013; Hetzinger et al., 2019). Therefore, while able to record SIC on an annual scale, *C. compactum*'s may be better suited to reconstruct SIC variability on a multi-year average scale (Hetzinger et al., 2019). The reasons for this likely are that other light inhibitors such as sedimentation, phytoplankton blooms and cloud cover may have affected the amplitude of algal anomalies for any given year. Therefore, 5-year running averages may smooth out the impact of these other light-related variables. Furthermore, 5-year running means of algal growth time series produced significant inter-series correlations at five sites, in comparison to 1 at an annual resolution (Figure 7). This suggested that either multi-year averages reduced individual noise and isolated the climate signal or that multi-year averages smoothed potential age model errors that may have reduced inter-series correlations at the annual level.

4.5. Inter-Sample Variability

In this study, all analyzed samples were included in calculating algal growth anomalies; however, the results clearly convey the variability between samples and that poor inter-series correlations may have affected the final algal correlation with sea ice conditions (Figure 6). B. Williams et al. (2014) suggested that inter-sample variability might be caused by variation in micro-environments (e.g., sample positioning relative to shading on the seafloor). On the other hand, Marali and Schöne (2015), who studied growth increments from the North Atlantic bivalve *Arctica islandica*, suggested that periods of low inter-annual variability could cause proxy time series from different samples to become desynchronized by factors affecting the organism at the individual level. Accordingly, Aasiaat and Qasigiannguit algal samples experienced reduced inter-annual summer SST variability (June–July) in recent record years. Simultaneously, higher inter-sample growth variability was observed (Figures 4 and S3 in Supporting Information S1). During low inter-annual climate variability, individual algal samples may be affected by differential predation pressures from chitons and urchins, physical disturbances, and competitive overgrowth may cause growth anomalies and consequent growth variability between samples (Adey et al., 2013). It is important to note that some samples produced synchronous algal growth anomalies, while the averaged inter-series correlation for the entire site was reduced significantly if a less synchronous sample was integrated in the average. Therefore, it will be important to focus on synchronous samples with a shared environmental signal when using *C. compactum* as a past sea ice proxy.

In this study, two to three samples per site were averaged, with the exception of Mosselbukta, where five samples were averaged (Figure S3 in Supporting Information S1). Sediment core-based studies often rely on a single well-dated core sample (e.g., Berben et al., 2017; Eiríksson et al., 2011). Coral-based proxy time series are also typically generated from a single core sample from each site (e.g., Calvo et al., 2007; Tierney et al., 2015) due to the high cost of geochemical analysis and time involved to prepare and process data (Corrège, 2006). However, multi-sample proxy studies are becoming more common to increase replication, proxy signal strength, and reliability (DeLong et al., 2013; Jones et al., 2009; von Reumont et al., 2016). Hetzinger et al. (2018) showed high replicability of Mg/Ca ratios down-sampled to 12 measurements/year from nine *C. compactum* samples collected in the Gulf of Maine, an ice-free region with larger growth increments, indicating their common climate signal. This theoretically suggests that only one algal sample could be used to build a time series. Conversely, colder and light-limited regions of the Arctic are more likely to produce thinner increments with unclear boundaries during high sea ice cover years which could introduce errors in age model construction. The results of 10-year running correlations at sites with long sea ice duration and high sea ice concentrations (i.e., Rigby Bay, Beechey Island, and Gulf of Boothia) showed a reduction in correlation with instrumental SIC and SST records further back in time, suggesting possible errors propagated later into the record due to the thinner increments more easily missed when growth rates are slower in high SIC and colder periods. The inclusion of more algal growth time series to strengthen the climate signal, similar to dendrochronology sample numbers, is only possible if the financial and time burdens of geochemical analysis are removed; recent tests with Mutvei staining suggest this possibility for the future as it may help more accurately measure annual increment widths (Siebert et al., 2020).

4.6. Outlooks and Recommendations

The *C. compactum* growth increment proxy is inextricably linked to factors that inhibit sunlight availability to the benthos, which can be multiple and variable depending on the sampling location. These include sea ice cover,

turbidity by sediment or algal blooms, and cloud cover, as well as other unassessed factors such as temporary overgrowth by macroalgae (i.e., kelp and other algae that might grow on the surface of *C. compactum*), snow cover thickness, sea ice thickness, water depth, and nutrient availability. Growth variability is also affected by temperature, which was especially noticeable at sites with low or no sea ice cover. Looking forward, one of *C. compactum*'s strengths as a short timescale climate archive (i.e., spanning a few centuries) is that it can capture recent climate change events such as the Little Ice Age and decadal anomalies such as the Atlantic Multidecadal Oscillation or Arctic Oscillation at a high resolution, events currently not fully resolved with high latitude marine sediment cores. Furthermore, additional comparisons with climate model hindcasts may indicate local variability only captured by the algal data. These future projects, however, should be tackled only after further investigating the inter-sample variability previously discussed with the integration of cross-dating methods.

5. Conclusions

This is the first multi-sample study investigating the relationship between algal anomalies of *C. compactum* (Mg/Ca, growth increment, and combined anomalies) and sea ice cover at multiple sites in the Arctic and Subarctic obtained from high spatial resolution satellite data sets. The results of this study showed that correlations between algal growth anomalies and sea ice concentration are stronger in regions/periods of higher sea ice concentrations, longer ice-on seasons, and reduced runoff and turbidity. Accordingly, our results yield important information for the identification of ideal study sites for future sea ice reconstructions. Annual algal growth anomalies may be sufficient, instead of combined algal anomalies or Mg/Ca ratios alone, to show the relative change in sea ice conditions at sites where algal anomalies respond more predictably to year-to-year sea ice variability. However, the algal growth proxy recorded SIC more strongly at most sites when downsampled to a 5-year running mean and may therefore produce better reconstructions on a multi-year average scale. Spatial correlation maps showed that algal growth anomalies generally inversely correlated to regional SIC variability at most sites. Weaker correlations between growth increment anomalies and sea ice conditions may be related to differential exposure, turbidity, and lengthening of the ice-free season in the past two decades, while correlations with sea ice cover in earlier, higher sea ice cover periods before 1979 were likely stronger (e.g., Hetzinger et al., 2019). Furthermore, algal growth anomalies from regions that experienced significant reductions in sea ice cover may shift from being sea ice dependent to being temperature dependent. Questions remain regarding variability between samples and their time series as some sites tended to have low inter-series correlations. Synchronous growth within sites should be a requirement to reconstruct annually-resolved sea ice conditions of the past. The significant correlations between algal growth anomalies and SIC highlight the opportunity *C. compactum* can provide as an in situ marine high-resolution ice cover proxy.

Conflict of Interest

The authors declare no conflicts of interest relevant to this study.

Data Availability Statement

This article contains original data and previously published data which are available in Halfar et al. (2013) and Hetzinger et al. (2019). All primary coralline red algae data sets are published through the NOAA National Centers for Environmental Information Paleoclimatology Data Repository (https://www.ncei.noaa.gov/access/paleo-search/study/34994). Primary data sets for this research are also included in figures and Supporting Information S1 files. Environmental data sets can be accessed through the following links: gridded sea ice concentrations https://nsidc.org/data/g02202; sea surface temperatures https://www.metoffice.gov.uk/hadobs/hadisst/; ice concentration imagery https://worldview.earthdata.nasa.gov; ice concentration imagery https://cryo.met.no/archive/ice-service/icecharts/quicklooks/; cloud fraction cover https://climexp.knmi.nl/; chlorophyll a concentrations https://giovanni.gsfc.nasa.gov.

Acknowledgments
Funding sources: NSERC Discovery (1303409; J.H.); NSERC CGS-D (CGSD3-518838 – 2018; N.L.). Kent Moore and Marc DeBenedetti for MATLAB assistance. Miriam Pfeiffer for statistical insights. Doritt Jacob for analytical work at Mainz University. Reviewers for encouraging and constructive remarks and suggestions.

References

Adey, W. H. (1965). The genus Clathromorphum (Corallinaceae) in the Gulf of Maine. *Hydrobiologia*, *26*(3–4), 539–573. https://doi.org/10.1007/bf00045545

Adey, W. H. (1970). The effects of light and temperature on growth rates in boreal-subarctic crustose corallines. *Journal of Phycology*, *6*(3), 269–276. https://doi.org/10.1111/j.1529-8817.1970.tb02392.x

Adey, W. H., Halfar, J., Humphreys, A., Suskiewicz, T., Belanger, D., Gagnon, P., & Fox, M. (2015). Subarctic rhodolith beds promote longevity of crustose coralline algal buildups and their climate archiving potential. *PALAIOS*, *30*(4), 281–293. https://doi.org/10.2110/palo.2014.075

Adey, W. H., Halfar, J., & Williams, B. (2013). *The coralline genus Clathromorphum Foslie emend Adey: Biological, physiological, and ecological factors controlling carbonate production in an Arctic-Subarctic climate archive*. Smithsonian Institution Scholarly Press.

Backman, J., Jakobsson, M., Løvlie, R., Polyak, L., & Febo, L. A. (2004). Is the central Arctic Ocean a sediment starved basin? *Quaternary Science Reviews*, *23*(11–13), 1435–1454. https://doi.org/10.1016/J.QUASCIREV.2003.12.005

Belmecheri, S., Namiotko, T., Robert, C., von Grafenstein, U., & Danielopol, D. L. (2009). Climate controlled ostracod preservation in Lake Ohrid (Albania, Macedonia). *Palaeogeography, Palaeoclimatology, Palaeoecology*, *277*(3–4), 236–245. https://doi.org/10.1016/J.PALAEO.2009.04.013

Belt, S. T. (2019). What do IP25 and related biomarkers really reveal about sea ice change? *Quaternary Science Reviews*, *204*, 216–219. https://doi.org/10.1016/J.QUASCIREV.2018.11.025

Belt, S. T., Brown, T. A., Rodriguez, A. N., Sanz, P. C., Tonkin, A., & Ingle, R. (2012). A reproducible method for the extraction, identification and quantification of the Arctic sea ice proxy IP25 from marine sediments. *Analytical Methods*, *4*(3), 705. https://doi.org/10.1039/c2ay05728j

Belt, S. T., Massé, G., Rowland, S. J., Poulin, M., Michel, C., & LeBlanc, B. (2007). A novel chemical fossil of palaeo sea ice: IP25. *Organic Geochemistry*, *38*(1), 16–27. https://doi.org/10.1016/J.ORGGEOCHEM.2006.09.013

Berben, S. M. P., Husum, K., Navarro-Rodriguez, A., Belt, S. T., & Aagaard-Sørensen, S. (2017). Semi-quantitative reconstruction of early to late Holocene spring and summer sea ice conditions in the northern Barents Sea. *Journal of Quaternary Science*, *32*(5), 587–603. https://doi.org/10.1002/jqs.2953

Bidle, K. D., & Azam, F. (1999). Accelerated dissolution of diatom silica by marine bacterial assemblages. *Nature*, *397*(6719), 508–512. https://doi.org/10.1038/17351

Burdett, H., Kamenos, N. A., & Law, A. (2011). Using coralline algae to understand historic marine cloud cover. *Palaeogeography, Palaeoclimatology, Palaeoecology*, *302*(1), 65–70. https://doi.org/10.1016/j.palaeo.2010.07.027

Butler, P. G., Scourse, J. D., Richardson, C. A., Wanamaker, A. D., Bryant, C. L., & Bennell, J. D. (2009). Continuous marine radiocarbon reservoir calibration and the 13C Suess effect in the Irish Sea: Results from the first multi-centennial shell-based marine master chronology. *Earth and Planetary Science Letters*, *279*(3–4), 230–241. https://doi.org/10.1016/j.epsl.2008.12.043

Calvo, E., Marshall, J. F., Pelejero, C., McCulloch, M. T., Gagan, M. K., & Lough, J. M. (2007). Interdecadal climate variability in the coral sea since 1708 A.D. *Palaeogeography, Palaeoclimatology, Palaeoecology*, *248*(1–2), 190–201. https://doi.org/10.1016/j.palaeo.2006.12.003

Cavalieri, D. J., & Parkinson, C. L. (2012). Arctic sea ice variability and trends, 1979-2010. *The Cryosphere*, *6*(4), 881–889. https://doi.org/10.5194/tc-6-881-2012, .

Chan, P., Halfar, J., Adey, W., Hetzinger, S., Zack, T., Moore, G. W. K., et al. (2017). Multicentennial record of Labrador Sea primary productivity and sea-ice variability archived in coralline algal barium. *Nature Communications*, *8*(1), 1–10. https://doi.org/10.1038/ncomms15543

Chan, P., Halfar, J., Williams, B., Hetzinger, S., Steneck, R., Zack, T., & Jacob, D. E. (2011). Freshening of the Alaska Coastal Current recorded by coralline algal Ba/Ca ratios. *Journal of Geophysical Research*, *116*(G1), G01032. https://doi.org/10.1029/2010JG001548

Comiso, J. C., Meier, W. N., & Gersten, R. (2017). Variability and trends in the Arctic Sea ice cover: Results from different techniques. *Journal of Geophysical Research: Oceans*, *122*(8), 6883–6900. https://doi.org/10.1002/2017JC012768

Corrège, T. (2006). Sea surface temperature and salinity reconstruction from coral geochemical tracers. *Palaeogeography, Palaeoclimatology, Palaeoecology*, *232*(2–4), 408–428. https://doi.org/10.1016/j.palaeo.2005.10.014

DeLong, K. L., Quinn, T. M., Taylor, F. W., Shen, C.-C., & Lin, K. (2013). Improving coral-base paleoclimate reconstructions by replicating 350 years of coral Sr/Ca variations. *Palaeogeography, Palaeoclimatology, Palaeoecology*, *373*, 6–24. https://doi.org/10.1016/j.palaeo.2012.08.019

De Vernal, A., Gersonde, R., Goosse, H., Seidenkrantz, M.-S., & Wolff, E. W. (2013). Sea ice in the paleoclimate system: The challenge of reconstructing sea ice from proxies—An introduction. *Quaternary Science Reviews*, *79*, 1–8. https://doi.org/10.1016/j.quascirev.2013.08.009

Ding, Q., Schweiger, A., L'Heureux, M., Battisti, D. S., Po-Chedley, S., Johnson, N. C., & , et al. (2017). Influence of high-latitude atmospheric circulation changes on summertime Arctic sea ice. *Nature Climate Change*, *7*, 289–295. https://doi.org/10.1038/nclimate3241

Eiríksson, J., Knudsen, K. L., Larsen, G., Olsen, J., Heinemeier, J., Bartels-Jónsdóttir, H. B., et al. (2011). Coupling of palaeoceanographic shifts and changes in marine reservoir ages off North Iceland through the last millennium. *Palaeogeography, Palaeoclimatology, Palaeoecology*, *302*(1–2), 95–108. https://doi.org/10.1016/j.palaeo.2010.06.002

Foster, M. S. (2001). Rhodoliths: Between rocks and soft places. *Journal of Phycology*, *37*(5), 659–667. https://doi.org/10.1046/j.1529-8817.2001.00195.x

Gemery, L., Cronin, T. M., Briggs, W. M., Brouwers, E. M., Schornikov, E. I., Stepanova, A., et al. (2017). An Arctic and Subarctic ostracode database: Biogeographic and paleoceanographic applications. *Hydrobiologia*, *786*(1), 59–95. https://doi.org/10.1007/s10750-015-2587-4

Glen Harrison, W., Yngve Børsheim, K., Li, W. K. W., Maillet, G. L., Pepin, P., Sakshaug, E., et al. (2013). Phytoplankton production and growth regulation in the subarctic North Atlantic: A comparative study of the Labrador Sea-Labrador/Newfoundland shelves and Barents/Norwegian/Greenland seas and shelves. *Progress in Oceanography*, *114*, 26–45. https://doi.org/10.1016/j.pocean.2013.05.003

Halfar, J., Adey, W. H., Kronz, A., Hetzinger, S., Edinger, E., & Fitzhugh, W. W. (2013). Arctic sea-ice decline archived by multicentury annual-resolution record from crustose coralline algal proxy. *Proceedings of the National Academy of Sciences of the United States of America*, *110*(49), 19737–19741. https://doi.org/10.1073/pnas.1313775110

Halfar, J., Williams, B., Hetzinger, S., Steneck, R. S., Lebednik, P., Winsborough, C., et al. (2011). 225 years of Bering Sea climate and ecosystem dynamics revealed by coralline algal growth-increment widths. *Geology*, *39*(6), 579–582. https://doi.org/10.1130/G31996.1

He, M., Hu, Y., Chen, N., Wang, D., Huang, J., & Stamnes, K. (2019). High cloud coverage over melted areas dominates the impact of clouds on the albedo feedback in the Arctic. *Scientific Reports*, *9*(1), 1–11. https://doi.org/10.1038/s41598-019-44155-w

Hetzinger, S., Halfar, J., Kronz, A., Simon, K., Adey, W. H., & Steneck, R. S. (2018). Reproducibility of *Clathromorphum compactum* coralline algal Mg/Ca ratios and comparison to high-resolution sea surface temperature data. *Geochimica et Cosmochimica Acta*, *220*, 96–109. https://doi.org/10.1016/j.gca.2017.09.044

Hetzinger, S., Halfar, J., Zack, T., Gamboa, G., Jacob, D. E., Kunz, B. E., et al. (2011). High-resolution analysis of trace elements in crustose coralline algae from the North Atlantic and North Pacific by laser ablation ICP-MS. *Palaeogeography, Palaeoclimatology, Palaeoecology*, *302*(1–2), 81–94. https://doi.org/10.1016/j.palaeo.2010.06.004

Hetzinger, S., Halfar, J., Zajacz, Z., Möller, M., & Wisshak, M. (2021). Late twentieth century increase in northern Spitsbergen (Svalbard) glacier-derived runoff tracked by coralline algal Ba/Ca ratios. *Climate Dynamics*, *56*, 3295–3303. https://doi.org/10.1007/s00382-021-05642-x

Hetzinger, S., Halfar, J., Zajacz, Z., & Wisshak, M. (2019). Early start of 20th-century Arctic sea-ice decline recorded in Svalbard coralline algae. *Geology*, *47*(10), 963–967. https://doi.org/10.1130/G46507.1

Hill, B. T., & Jones, S. J. (1990). The Newfoundland ice extent and the solar cycle from 1860 to 1988. *Journal of Geophysical Research*, *95*(C4), 5385. https://doi.org/10.1029/JC095iC04p05385

Howell, S. E. L., Duguay, C. R., & Markus, T. (2009). sea ice conditions and melt season duration variability within the Canadian Arctic Archipelago: 1979–2008. *Geophysical Research Letters*, *36*(10). https://doi.org/10.1029/2009GL037681

Jones, P. D., Briffa, K. R., Osborn, T. J., Lough, J. M., Van Ommen, T. D., Vinther, B. M., et al. (2009). High-resolution palaeoclimatology of the last millennium: a review of current status and future prospects. *The Holocene*, *19*(1), 3–49. https://doi.org/10.1177/0959683608098952

Kaufman, D. S. (2009). An overview of late Holocene climate and environmental change inferred from Arctic lake sediment. *Journal of Paleolimnology*, *41*(1), 1–6. https://doi.org/10.1007/s10933-008-9259-6

Kinnard, C., Zdanowicz, C. M., Fisher, D. A., Isaksson, E., de Vernal, A., & Thompson, L. G. (2011). Reconstructed changes in Arctic sea ice over the past 1,450 years. *Nature*, *479*, 509–512. https://doi.org/10.1038/nature10581

Knies, J., Cabedo-Sanz, P., Belt, S. T., Baranwal, S., Fietz, S., & Rosell-Melé, A. (2014). The emergence of modern sea ice cover in the Arctic Ocean. *Nature Communications*, *5*(11), 1–7. https://doi.org/10.1038/ncomms6608

Köseoğlu, D., Belt, S. T., Husum, K., & Knies, J. (2018). An assessment of biomarker-based multivariate classification methods versus the PIP25 index for paleo Arctic sea ice reconstruction. *Organic Geochemistry*, *125*, 82–94. https://doi.org/10.1016/j.orggeochem.2018.08.014

Kucera, M., Weinelt, M., Kiefer, T., Pflaumann, U., Hayes, A., Weinelt, M., et al. (2005). Reconstruction of sea-surface temperatures from assemblages of planktonic foraminifera: Multi-technique approach based on geographically constrained calibration data sets and its application to glacial Atlantic and Pacific oceans. *Quaternary Science Reviews*, *24*, 951–998. https://doi.org/10.1016/j.quascirev.2004.07.014

Lang, C., Fettweis, X., & Erpicum, M. (2015). Stable climate and surface mass balance in Svalbard over 1979-2013 despite the Arctic warming. *The Cryosphere*, *9*(1), 83–101. https://doi.org/10.5194/tc-9-83-2015

Mahoney, A. R., Bockstoce, J. R., Botkin, D. B., Eicken, H., & Nisbet, R. A. (2011). Sea-Ice distribution in the Bering and Chukchi seas: Information from historical whaleships' logbooks and journals. *Arctic*, *64*(4), 465–477. Retrieved from http://www.jstor.org/stable/41319241

Marali, S., & Schöne, B. R. (2015). Oceanographic control on shell growth of Arctica islandica (Bivalvia) in surface waters of Northeast Iceland—Implications for paleoclimate reconstructions. *Palaeogeography, Palaeoclimatology, Palaeoecology*, *420*, 138–149. https://doi.org/10.1016/j.palaeo.2014.12.016

Massicotte, P., Amiraux, R., Amyot, M. P., Archambault, P., Ardyna, M., Arnaud, L., et al. (2020). Green edge ice camp campaigns: Understanding the processes controlling the under-ice arctic phytoplankton spring bloom. *Earth System Science Data*, *12*(1), 151–176. https://doi.org/10.5194/essd-12-151-2020

Meier, W. N., Fetterer, F., Savoie, M., Mallory, S., Duerr, R., & Stroeve, J. (2017). *NOAA/NSIDC climate data record of passive microwave sea ice concentration*. NSIDC: National Snow and Ice Data Center. https://doi.org/10.7265/N59P2ZTG

Meier, W. N., Hovelsrud, G. K., Van Oort, B. E. H., Key, J. R., Kovacs, K. M., Michel, C., et al. (2014). Arctic sea ice in transformation: A review of recent observed changes and impacts on biology and human activity. *Reviews of Geophysics*, *52*(3), 185–217. https://doi.org/10.1002/2013RG000431

Melling, H. (2002). Sea ice of the northern Canadian Arctic Archipelago. *Journal of Geophysical Research: Oceans*, *107*(C11). https://doi.org/10.1029/2001jc001102

Möller, M., & Kohler, J. (2018). Differing climatic mass balance evolution across Svalbard glacier regions over 1900–2010. *Frontiers in Earth Science*, *6*, 128. https://doi.org/10.3389/feart.2018.00128

Müller, J., Wagner, A., Fahl, K., Stein, R., Prange, M., & Lohmann, G. (2011). Towards quantitative sea ice reconstructions in the northern North Atlantic: A combined biomarker and numerical modelling approach. *Earth and Planetary Science Letters*, *306*(3–4), 137–148. https://doi.org/10.1016/J.EPSL.2011.04.011

National Center for Atmospheric Research Staff (Eds). (2019). The climate data guide: Sea ice concentration data from NOAA OI. Retrieved from https://climatedataguide.ucar.edu/climate-data/sea-ice-concentration-data-noaa-oi

Østby, T. I., Vikhamar Schuler, T., Ove Hagen, J., Hock, R., Kohler, J., & Reijmer, C. H. (2017). Diagnosing the decline in climatic mass balance of glaciers in Svalbard over 1957-2014. *The Cryosphere*, *11*(1), 191–215. https://doi.org/10.5194/tc-11-191-2017

Paillard, D., Labeyrie, L., & Yiou, P. (1996). Macintosh program performs time-series analysis. *Eos, Transactions American Geophysical Union*, *77*(39), 379. https://doi.org/10.1029/96eo00259

Peng, G., Meier, W. N., Scott, D. J., & Savoie, M. H. (2013). A long-term and reproducible passive microwave sea ice concentration data record for climate studies and monitoring. *Earth System Science Data*, *5*(2), 311–318. https://doi.org/10.5194/essd-5-311-2013

Polyak, L., Alley, R. B., Andrews, J. T., Brigham-Grette, J., Cronin, T. M., Darby, D. A., et al. (2010). History of sea ice in the Arctic. *Quaternary Science Reviews*, *29*(15–16), 1757–1778. https://doi.org/10.1016/j.quascirev.2010.02.010

Ran, L., Jiang, H., Knudsen, K. L., & Eiríksson, J. (2011). Diatom-based reconstruction of palaeoceanographic changes on the North Icelandic shelf during the last millennium. *Palaeogeography, Palaeoclimatology, Palaeoecology*, *302*(1–2), 109–119. https://doi.org/10.1016/j.palaeo.2010.02.001

Rayner, N. A., Parker, D. E., Horton, E. B., Folland, C. K., Alexander, L. V., Rowell, D. P., et al. (2003). Global analyses of sea surface temperature, sea ice, and night marine air temperature since the late nineteenth century. *Journal of Geophysical Research*, *108*(D14). https://doi.org/10.1029/2002JD002670

Reynolds, R. W., Rayner, N. A., Smith, T. M., Stokes, D. C., & Wang, W. (2002). An improved in situ and satellite SST analysis for climate. *Journal of Climate*, *15*(13), 1609–1625. https://doi.org/10.1175/1520-0442(2002)015<1609:aiisas>2.0.co;2

Seidenkrantz, M.-S. (2013). Benthic foraminifera as palaeo sea-ice indicators in the subarctic realm – examples from the Labrador Sea–Baffin Bay region. *Quaternary Science Reviews*, *79*, 135–144. https://doi.org/10.1016/J.QUASCIREV.2013.03.014

Sexton, P. F., & Wilson, P. A. (2009). Preservation of benthic foraminifera and reliability of deep-sea temperature records: Importance of sedimentation rates, lithology, and the need to examine test wall structure. *Paleoceanography*, *24*(2). https://doi.org/10.1029/2008PA001650

Sicre, M. A., Jacob, J., Ezat, U., Rousse, S., Kissel, C., Yiou, P., et al. (2008). Decadal variability of sea surface temperatures off North Iceland over the last 2000 years. *Earth and Planetary Science Letters*, *268*(1–2), 137–142. https://doi.org/10.1016/j.epsl.2008.01.011

Sicre, M. A., Yiou, P., Eiríksson, J., Ezat, U., Guimbaut, E., Dahhaoui, I., et al. (2008). A 4500-year reconstruction of sea surface temperature variability at decadal time-scales off North Iceland. *Quaternary Science Reviews*, *27*(21–22), 2041–2047. https://doi.org/10.1016/j.quascirev.2008.08.009

Siebert, V., Poitevin, P., Chauvaud, L., Schöne, B. R., Lazure, P., & Thébault, J. (2020). Using growth and geochemical composition of Clathromorphum compactum to track multiscale North Atlantic hydro-climate variability. *Palaeogeography, Palaeoclimatology, Palaeoecology*, *562*, 110097. https://doi.org/10.1016/j.palaeo.2020.110097

Stein, R., & Fahl, K. (2013). Biomarker proxy shows potential for studying the entire Quaternary Arctic sea ice history. *Organic Geochemistry*, *55*, 98–102. https://doi.org/10.1016/J.ORGGEOCHEM.2012.11.005

Stein, R., Fahl, K., Schreck, M., Knorr, G., Niessen, F., Forwick, M., et al. (2016). Evidence for ice-free summers in the late Miocene central Arctic Ocean. *Nature Communications*, *7*, 11148. https://doi.org/10.1038/ncomms11148

Teichert, S., & Freiwald, A. (2014). Polar coralline algal CaCO3-production rates correspond to intensity and duration of the solar radiation. *Biogeosciences*, *11*(3), 833–842. https://doi.org/10.5194/bg-11-833-2014

Tierney, J. E., Abram, N. J., Anchukaitis, K. J., Evans, M. N., Giry, C., Kilbourne, K. H., et al. (2015). Tropical sea surface temperatures for the past four centuries reconstructed from coral archives. *Paleoceanography*, *30*(3), 226–252. https://doi.org/10.1002/2014PA002717

van Pelt, W. J. J., Kohler, J., Liston, G. E., Hagen, J. O., Luks, B., Reijmer, C. H., & Pohjola, V. A. (2016). Multidecadal climate and seasonal snow conditions in Svalbard. *Journal of Geophysical Research: Earth Surface*, *121*(11), 2100–2117. https://doi.org/10.1002/2016JF003999

von Reumont, J., Hetzinger, S., Garbe-Schönberg, D., Manfrino, C., & Dullo, W.-C. (2016). Impact of warming events on reef-scale temperature variability as captured in two Little Cayman coral Sr/Ca records. *Geochemistry, Geophysics, Geosystems*, *17*(3), 846–857. https://doi.org/10.1002/2015GC006194

Walsh, J. E., Fetterer, F., Stewart, S. J., & Chapman, W. L. (2017). A database for depicting Arctic sea ice variations back to 1850. *Geographical Review*, *107*(1), 89–107. https://doi.org/10.1111/j.1931-0846.2016.12195.x

Warn-Varnas, A., Allard, R., & Piacsek, S. (1991). Synoptic and seasonal variations of the ice-ocean circulation in the Arctic: A numerical study. *Annals of Glaciology*, *15*, 54–62. https://doi.org/10.1017/s026030550000954x

Wang, M., & Overland, J. E. (2012). Projected future duration of the sea-ice-free season in the Alaskan Arctic. *Progress in Oceanography*, *136*, 50–59. https://doi.org/10.1029/2012GL052868

Williams, B., Halfar, J., DeLong, K. L., Hetzinger, S., Steneck, R. S., & Jacob, D. E. (2014). Multi-specimen and multi-site calibration of Aleutian coralline algal Mg/Ca to sea surface temperature. *Geochimica et Cosmochimica Acta*, *139*, 190–204. https://doi.org/10.1016/j.gca.2014.04.006

Williams, S., Adey, W. H., Halfar, J., Kronz, A., Gagnon, P., Bélanger, D., & Nash, M. (2018). Effects of light and temperature on Mg uptake, growth, and calcification in the proxy climate archive *Clathromorphum compactum*. *Biogeosciences*, *15*(19), 5745–5759. https://doi.org/10.5194/bg-15-5745-2018

Worley, S. J., Woodruff, S. D., Reynolds, R. W., Lubker, S. J., & Lott, N. (2005). ICOADS Release 2.1 data and products. *Internaltional Journal of Climatology*, *25*, 823–842. https://doi.org/10.1002/joc.1166